Mechanism of Acid Dissociation in Water Clusters: Electronic Structure Studies of $(H_2O)_nHX$ ($n = 4, 7$; X = OH, F, HS, HSO_3, $OOSO_2H$, $OOH \cdot SO_2$)

Angela Smith, Mark A. Vincent, and Ian H. Hillier*

Department of Chemistry, University of Manchester, Manchester, M13 9PL, United Kingdom

Received: October 27, 1998; In Final Form: December 19, 1998

High-level electronic structure calculations have been carried out to identify stationary structures on the potential energy surface of a number of acids in water clusters, with 4 or 7 solvent molecules. The calculations employed a 6-311++g** basis with correlation at the MP2 and DFT (B3LYP) levels. Both DFT and a smaller basis set tended to favor the zwitterionic, compared to the unionized, structures. The cooperative nature of the ionization process was especially evident, with single and double layers of three water molecules separating the ionized groups and actively participating in ionization. For the pure water clusters, both $(H_2O)_5$ and $(H_2O)_8$ had similar relative energies for unionized, zwitterionic, and transition-state structures, showing that a range of structures and ionization mechanisms can occur in bulk water. For HF and H_2S, the relative energetics and stationary structures showed ionization to be more favorable in the larger clusters. The trend of earlier transition states for the stronger acids was identified for HF, H_2S, and H_2SO_3.

Introduction

Water plays a central role in understanding chemical processes in the condensed phase. For this reason, there are ongoing attempts to model, at a realistic level, both structural and energetic aspects of the effect of water on chemical reactions. Such models must of necessity include quantum chemical descriptions of bond breakage and formation, although a molecular mechanical description of those solvent molecules not directly involved in the reaction may be employed as in hybrid quantum mechanical/molecular mechanical methods.

Solutes in small water clusters, rather than in the bulk, are being increasingly studied.[1] They are of interest in their own right[2] but also have direct applications, since reactions important in atmospheric and combustion chemistry take place in such clusters.[3] Furthermore, clusters of specific size are often amenable to experimental study.[4] They can also provide a way of identifying effects important in the bulk and in developing and testing models applicable to the bulk, such as studying force fields and polarization effects.

To date, there have been many theoretical studies on purely water clusters[5−17] and clusters containing a small solute,[18−24] focusing on minimum energy structures. A large number of studies of the structure and energetics of increasingly large water clusters have been reported, using both ab initio and force field methods. Here both ring (**1a**) and cluster (**1b**) structures may be formed. For small numbers of water molecules, ($(H_2O)_n$, $n \leq 5$) the ring is preferred, with the transition to the cluster motif taking place for $n > 5$.[10,25−27] Similarly, both ring and cluster structures are possible when a solute (HX) replaces a water molecule in the complex. There is increasing interest in the structure and indeed reactivity of solutes in water clusters. Thus, for example, the question as to whether halide ions reside on the surface or in the interior of small water clusters has not been completely resolved,[28−31] and there is interest in the stability of neutral and zwitterionic forms of such clusters containing acidic or basic solutes.[7,8,22−24] In the area of reactivity, high-level electronic structure methods can be used to model stationary structures, both minima and transition states, as exemplified by our recent study of SO_2 oxidation by H_2O_2 in water clusters, leading to species implicated in acid rain formation.[32] The important goal of properly modeling reactions in the bulk aqueous phase is now being tackled, for example, by molecular dynamics employing a quantum mechanical potential within a planewave formalism as pioneered by Car and Parrinello.[33]

The role of the work described in this paper is to further contribute to our understanding of prototype reactions in water clusters by using quantum mechanical methods to identify stationary structures including transition states for such reactions. We report calculations on a variety of both solutes and cluster sizes to study reactions involving water itself, the small solutes HCl, HF, and H_2S, and the larger solutes H_2SO_3 and related species. The structures studied are exemplified in Figure 1. The calculations, carried out using Gaussian 94,[34] employed a large Gaussian basis set (6-311++g**) with correlation included using both MP2 and density functional theory (DFT) methods with a B3LYP functional. For the larger systems, computational expense restricts these studies to DFT calculations. All stationary structures were characterized as minima or transition states by calculation of their harmonic vibrational frequencies. Free energies were calculated within the perfect gas, rigid rotor, harmonic oscillator approximation at 298 K.

Computational Results

Water Clusters $(H_2O)_5$, $(H_2O)_8$. Water clusters have been extensively studied using high-level electronic structure methods. For clusters constructed from neutral water molecules, DFT calculations employing a number of functionals have given results in good agreement with MP2 studies.[12] Correlation effects beyond second order have been shown to be unimportant in describing water clusters.[11] In previous studies, quite large basis sets of double, triple, and quadruple-ζ quality for the valence orbitals, along with polarization functions, have been employed.[9] Recent papers have also addressed the question of ion pair formation in water clusters to shed light on the dissociation

10.1021/jp984216n CCC: $18.00

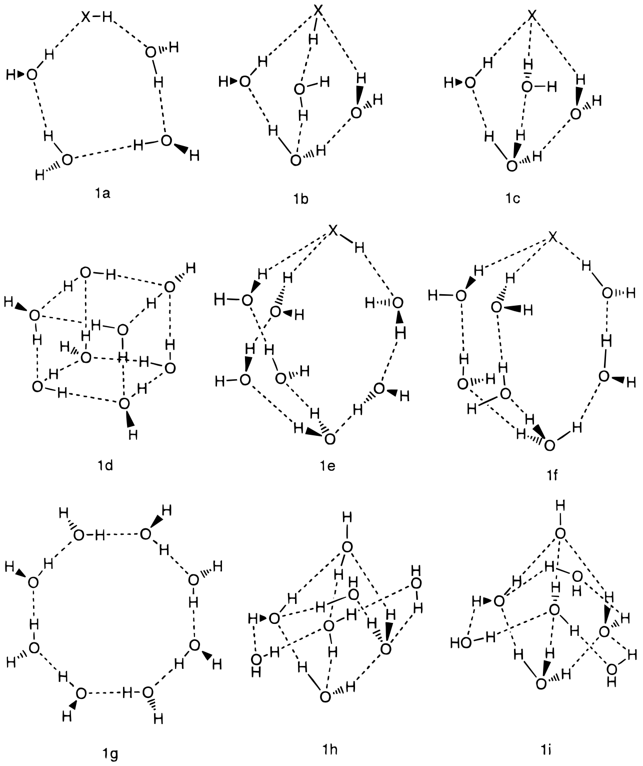
1a 1b 1c 1d 1e 1f 1g 1h 1i

Figure 1. Minimum energy structures considered.

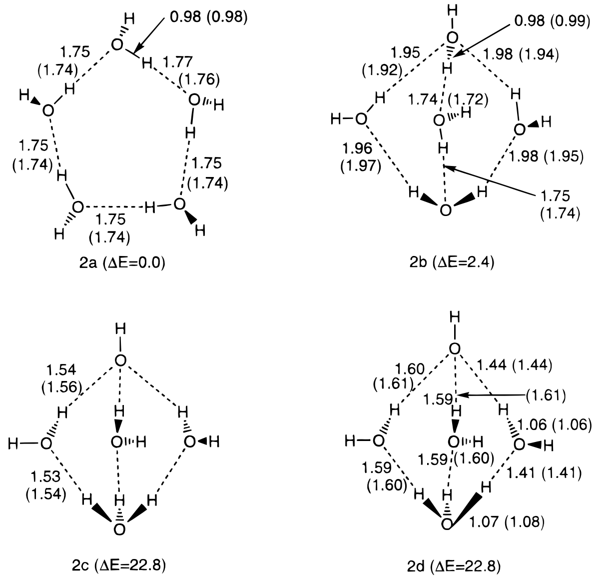

2a (ΔE=0.0) 2b (ΔE=2.4) 2c (ΔE=22.8) 2d (ΔE=22.8)

Figure 2. Stationary structures of $(H_2O)_4$ H_2O at MP2 and (in brackets) B3LYP levels. The MP2 results for **2b** and **2c** are from ref 35. In this, and subsequent figures, distances are in angstroms, and relative energies (kcal mol^{-1}) are given at the MP2//B3LYP level.

mechanism of H_2O in bulk water,[7,8,15,35] which has also been addressed by first-principles molecular dynamics studies.[33] We have studied clusters of five and eight water molecules, since structures of this size permit important cooperative effects to be investigated. The minimum energy structures that we have located (Figures 2−4) and their relative energies (Table 1) are in broad agreement with previous studies. We note that the structures of both minima and transition states differ little at the MP2 and B3LYP levels, which gives us confidence to use the DFT method to explore the larger systems. For the water pentamer, we find the ring structure (**2a**) to be the more stable than the cluster (**2b**) by ∼3 kcal mol^{-1}. The ion pair structure (**2c**) in which the H_3O^+ and OH^- ions are separated by a single layer of water molecules is also an energy minimum, some 20−25 kcal mol^{-1} higher in energy than the pentamer ring structure. The corresponding transition state (**2d**) is close to the ion pair, both in energy and structure, having a well developed hydroxonium ion and a barrier of <1 kcal mol^{-1} with respect to the ion pair minimum. The important role of the layer of three water molecules that separate the developing OH^- and H_3O^+ species is evident from the transition state (**2d**) and ion pair (**2c**) structures. One water molecule actively participates in a proton shuttle mechanism, while the other two water molecules move to stabilize the developing charges.

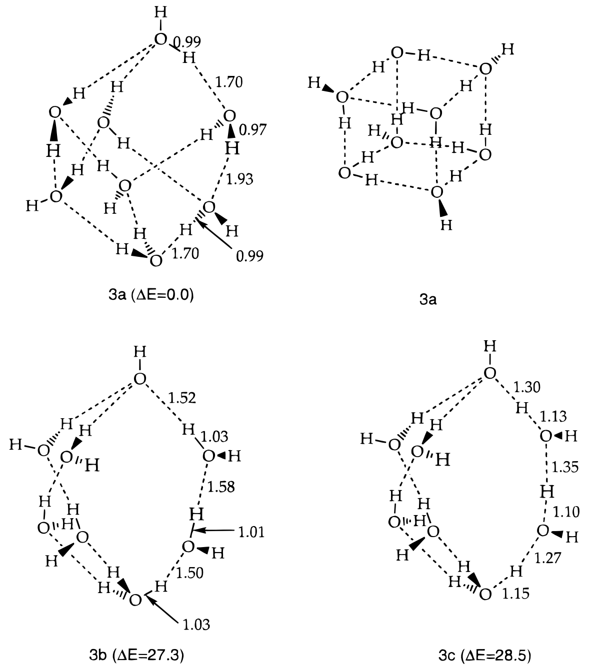

3a (ΔE=0.0) 3a 3b (ΔE=27.3) 3c (ΔE=28.5)

Figure 3. Stationary structures of $(H_2O)_7$ H_2O at the B3LYP level.

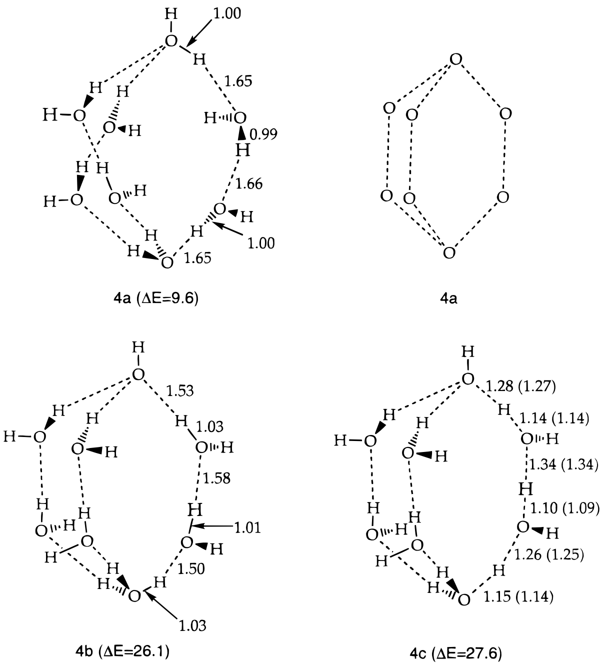

4a (ΔE=9.6) 4a 4b (ΔE=26.1) 4c (ΔE=27.6)

Figure 4. Stationary structures of $(H_2O)_7$ H_2O at the B3LYP and (in brackets) MP2 levels.

Both the way of including electron correlation and the inclusion of zero-point and thermodynamic corrections affect

TABLE 1: Relative Energies (kcal mol^{-1}) of $(H_2O)_n$ Species

		MP2//MP2		MP2//B3LYP	B3LYP//B3LYP	
		ΔE	ΔG	ΔE	ΔE	ΔG
				$(H_2O)_5$		
ring	(**2a**)	0.0[a]	0.0[a]	0.0	0.0	0.0
cluster	(**2b**)	2.3[a]	3.2[a]	2.4	3.1	4.8
ion pair	(**2c**)	22.7[a]	24.9[a]	22.8	20.9	23.4
transition state	(**2d**)	22.8	24.9	22.8	21.0	23.3
				$(H_2O)_8$		
cube	(**3a**)			0	0	0
ion pair	(**3b**)			27.3	24.0	17.9
transition state	(**3c**)			28.5	25.3	16.4
diamond	(**4a**)			9.6	8.7	0.9
ion pair	(**4b**)			26.1	22.4	16.4
transition state	(**4c**)			27.6	23.9	15.3
trisolvated	(**1h**)			11.3	13.0	7.2
ion pair	(**1i**)			32.4	32.1	26.1
ring	(**1g**)			12.5	10.5	−1.3

[a] Data from ref 35.

TABLE 2: Relative Energies (kcal mol^{-1}) of $(H_2O)_4HCl$ Species

		MP2//B3LYP	B3LYP//B3LYP	
		ΔE	ΔE	ΔG
		$(H_2O)_4HCl$		
ring	(**5a**)	0	0	0
ion pair	(**5b**)	1.0	−1.4	3.7

the relative energies of the stationary points on the $H_{10}O_5$ potential energy surface. Compared to MP2, the B3LYP functional underestimates both the energy difference between the cluster and ion pair and the barrier for dissociation, by 2−3 kcal mol^{-1}. Thermodynamic corrections increase both these quantities, but by a somewhat smaller amount (Table 1).

In the ion pair structure arising from the water pentamer (**2c**), the two ions are separated by a layer of three water molecules. To approach further the actual bulk situation we have studied the water octamer, which allows for the possibility of the positive and negative ions to be separated by two water layers. We have investigated four structures of $(H_2O)_8$, cube (**3a**), diamond (**4a**), ring (**1g**) and our previous water pentamer cluster solvated by three additional water molecules, one hydrogen bonded to each of the water molecules in the layer separating the reactive pair (**1h**). Of these four, the cube is by far the most stable (Table 1), by ∼10 kcal mol^{-1}, compared to the three other structures. However, due mainly to the relatively large zero-point energy of the cube structure, arising from the optimal arrangement of hydrogen bonds, the free energy difference between the four structures is quite small. The cube is still favored over the diamond structure but now by only 0.9 kcal mol^{-1}, while the ring structure has a lower free energy than the cube (by 1.3 kcal mol^{-1}). Both an ion pair structure and the corresponding transition state that arise from the cube (**3b**, **3c**) and diamond (**4b**, **4c**) water octamers have been located. Each of the two transition states and the two zwitterionic minima have essentially the same bond lengths. However, they are distinct stationary structures that differ in the orientation of the dangling hydrogen atoms of the intermediate layers of water molecules. The two transition states are earlier than that for the water pentamer (**2d**) and thus do not show such a well-developed hydroxonium ion. The shuttle mechanism for proton transfer is clearly evident in the two octamer transition structures in which the transferring proton is involved in a distorted $H_5O_2^+$ rather than a H_3O^+ species. Indeed, the definite O−H bond length alternation in the chain between the developing OH^- and H_3O^+ clearly shows how proton transfer can take place over long distances. To check this important finding, the transition state (**4c**) was located at the MP2 level. This structure is essentially the same as that found using the B3LYP functional. However, as was found for the pentamer, in the case of the octamer the energy needed to form the ion pair is again underestimated at the B3LYP level, when compared to the MP2 value. For the cube structure, which leads to the ion pair via the transition state (**3c**), a free energy increase to form the ion pair is estimated at the MP2 level to be 21.2 kcal mol^{-1}, using the thermodynamic corrections obtained at the B3LYP level.

It is interesting to compare the results of our calculations and previous studies of the energy difference between the neutral and zwitterion minima with the experimental free energy difference of 21.4 kcal mol^{-1}, based upon $K_w = 10^{-14}$. Taking the pentamer results first, use of the cluster structure for the unionized state leads to a free energy difference at the MP2 level of 21.7 kcal mol^{-1}, in excellent agreement with experiment. The corresponding value for the octamer, 21.2 kcal mol^{-1}, is essentially the same. Both values are smaller at the DFT (B3LYP) level, being 18.6 and 17.9 kcal mol^{-1} for the pentamer and octamer, respectively, and we have found that it is further reduced (to 16.4 kcal mol^{-1} for the pentamer structure) with the BLYP functional. Thus taking the MP2 results to be the most accurate, it would appear that the commonly used BLYP functional underestimates the energy difference between the neutral and the zwitterionic forms by ∼5 kcal mol^{-1}. It is noteworthy that first principle molecular dynamics studies, which do utilize a BLYP functional, underestimate this energy difference by 4.1 kcal mol^{-1} when compared to experiment.[33]

It is worth highlighting again the similar energetics for proton transfer in the two different sized clusters that we have studied. This shows that a wide range of structures are to be expected in bulk water, particularly with respect to the separation of the two ionic species present.

$(H_2O)_4HCl$, $(H_2O)_7HCl$. The atmospheric importance of the interaction of HCl with liquid water and ice[36] has prompted many studies of water−HCl clusters.[18−24] It is well recognized that, in small clusters, the most stable structures involve unionized HCl, while for larger clusters, the zwitterionic form is favored, with the transition between the two structures occurring for clusters involving four water molecules. For such clusters, at the B3LYP level, we have identified two minimum energy structures, the neutral ring (**5a**) and the ion pair (**5b**) (Table 2). These structures are close in energy, with the most stable one being dependent on the level of correlation employed and whether finite temperature corrections are included. The DFT treatment tends to favor the ion pair, while MP2 favors the ring structure, with thermodynamic effects also favoring the ring structure. In the ring structure involving neutral HCl, the H−Cl bond length (1.37 Å) is noticeably greater than that in free H−Cl (1.29 Å at B3LYP/6-311++g**), showing the very strong acid nature of HCl. Associated with this are short hydrogen bond lengths (1.53, 1.68 Å) involving the interaction of the neighboring water molecule, both with HCl itself and with the next water molecule in the ring (**5a**). These short lengths are indicative of incipient HCl ionization and formation of a neighboring hydroxonium ion.

In view of the closeness of the energies of these neutral and ionic forms of $HCl(H_2O)_4$, we have explored the effect of different descriptions of electron correlation, and enlarged basis sets on the optimal predicted structures. For computational economy, we have chosen to investigate the smaller system $HCl(H_2O)_3$ where Re et al.[22] have identified an ionic cluster (Figure 5d) as an energy minimum some 6 kcal mol^{-1} above the preferred structure involving unionized HCl (Figure 5e). Their

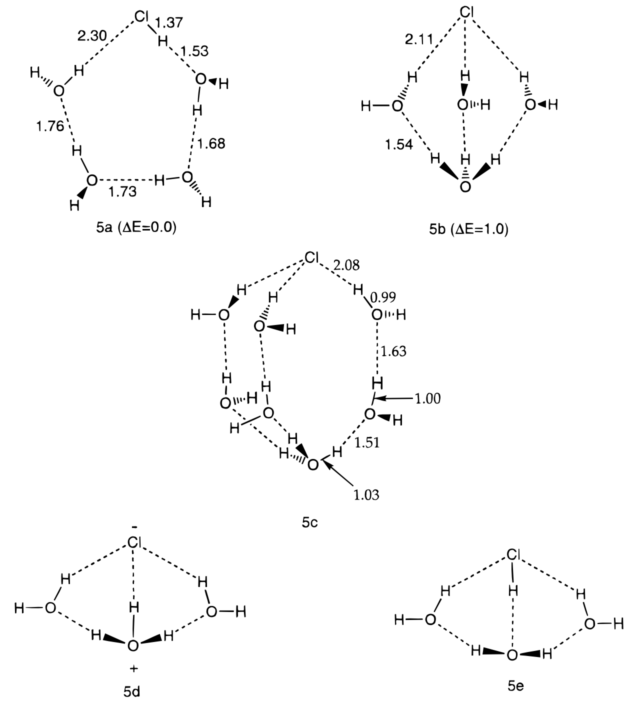

Figure 5. Stationary structures of $(H_2O)_n$ HCl at the B3LYP level.

calculations were carried out at the B3LYP/D95++(p,d) and B3LYP/D95(p,d) levels. To compare electron correlation using MP2 and B3LYP treatments, we have optimized at the MP2/D95++(p,d) level, starting with the ionic form from the B3LYP/D95++(p,d) calculation. This structure collapsed to the neutral one shown in Figure 5. This result suggests that the DFT model preferentially favors the ionic rather than the neutral form, in line with our results for $(H_2O)_4H_2O$. However, with the basis we have used throughout this study, 6-311++g**, and using the B3LYP functional, we again found only the neutral rather than the ionic form (Figure 5d). This basis is somewhat more flexible than D95++g**, having an extra set of p and s functions.

To examine the effect of increasing the size of the cluster to approach more complete solvation, we have studied a cluster involving HCl and seven water molecules. As in the four water case, no cluster structure involving unionized HCl could be located. The ion pair structure found is shown in Figure 5c. When compared to $H_9O_4^+$ Cl^-, $H_{15}O_7^+$ Cl^- has shorter hydrogen bonds to Cl^- (2.08 Å compared to 2.11 Å) and to H_3O^+ (1.51 Å compared to 1.54 Å). Also of note is the short hydrogen bond (1.63 Å) between the pairs of bridging waters. These values again show the important role of the bridging waters in stabilizing the ion pair.

$(H_2O)_4$HF, $(H_2O)_7$HF. For the complex involving HF and four water molecules, four stationary structures were identified (Figure 6), similar to those found for the water pentamer. Both the ring (**6a**) and the cluster (**6b**) structure involving neutral HF show considerably greater solute−solvent interactions than the corresponding ones for $(H_2O)_5$. Thus, in the ring and cluster structures of $(H_2O)_4$ HF, the hydrogen bond distance to the hydrogen of HF is 1.50 and 1.46 Å, respectively, compared to the corresponding values of 1.76 and 1.72 Å in $(H_2O)_5$ (Figure 2a,b). On solvation by four water molecules, the H−F bond has lengthened, being 0.98 and 0.99 Å in the ring and cluster, compared to the value of 0.92 Å in free HF.

The structure of the ion pair $H_9O_4^+$ F^- (Figure 6c) is remarkably similar to that of the corresponding water pentamer, $H_9O_4^+$ OH^- (Figure 2c). The corresponding transition states linking the cluster and the ion pair (Figures 2d and 6d) are also similar, although that for $H_9O_4^+$ F^- is further from the zwitterionic minimum than is the case for $H_9O_4^+$ OH^-, reflecting the greater basicity of OH^- compared to F^-. This effect is also evident in the barrier to the reaction being 0.4 kcal mol^{-1} with respect to the ion pair (Table 3), compared to 0.1 kcal mol^{-1} for the corresponding water pentamer. It is of interest to note that upon inclusion of zero-point and thermodynamic corrections, the free energy of the transition state is reduced to a value below that of the ion pair.

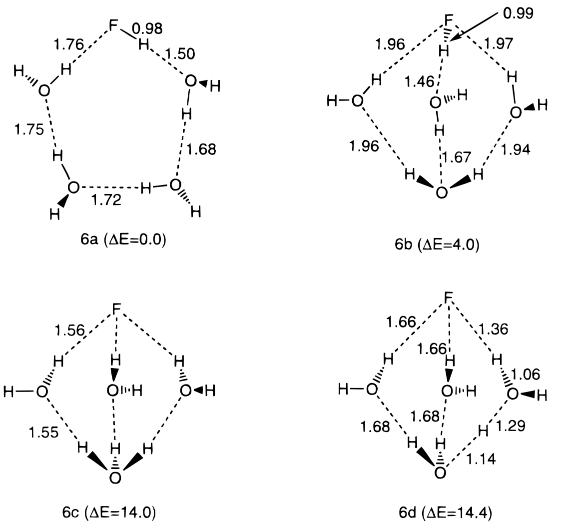

Figure 6. Stationary structures of $(H_2O)_4$ HF at the B3LYP level.

TABLE 3: Relative Energies (kcal mol^{-1}) of $(H_2O)_n$HF Species

		MP2//B3LYP	B3LYP//B3LYP	
		ΔE	ΔE	ΔG
		$(H_2O)_4$HF		
ring	(**6a**)	0	0	0
cluster	(**6b**)	4.0	4.5	5.3
ion pair	(**6c**)	14.0	10.9	14.2
transition state	(**6d**)	14.4	11.5	13.3
		$(H_2O)_7$HF		
cluster	(**7a**)	0	0	0
ion pair	(**7b**)	3.8	0.9	3.9
transition state	(**7c**)	6.9	4.3	3.7

The effect of further solvation of HF is evident in the predicted stationary structures of $(H_2O)_7$ HF shown in Figure 7. The additional three water molecules have had a noticeable effect on the structure of HF and the three water molecules that interact directly with it. Thus, the H−F bond has lengthened by 0.03 Å and the hydrogen bonds to three nearest water molecules have shortened by 0.09 Å, when compared to $(H_2O)_4$ HF. This shows the important longer range effects of the more distant water molecules. This effect is also evident in the ion pair structure with the F^- distance to neighboring waters being reduced by 0.04 Å upon inclusion of the more distant water molecules. The overall effect of the second solvation shell is to reduce the separation of the ion pair and neutral species from 8.9 kcal mol^{-1} for four water molecules to 3.9 kcal mol^{-1} in the larger cluster (Table 3). This is reflected in the transition-state structure (**7c**), which is considerably earlier than that for $(H_2O)_4$ HF.

$(H_2O)_4$ H_2S, $(H_2O)_7H_2S$. The results for $(H_2O)_4$ H_2S shown in Figure 8, where three minimum energy structures and one transition state have been located, parallel those found for $(H_2O)_4$ H_2O, with the quantitative differences reflecting the stronger

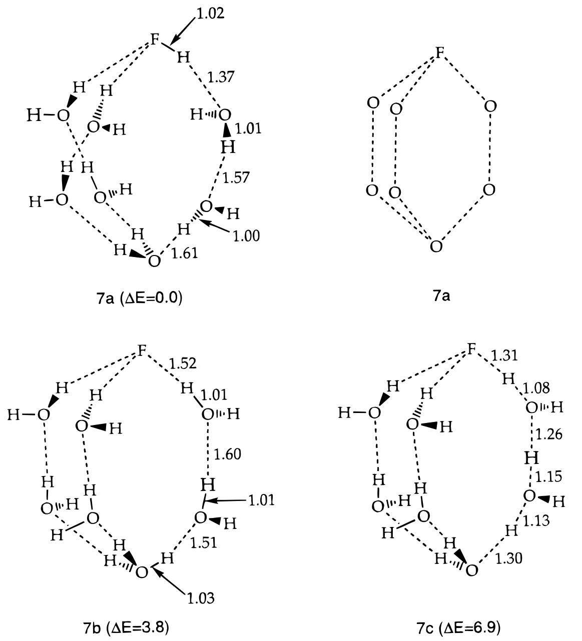

7a (ΔE=0.0) 7a

7b (ΔE=3.8) 7c (ΔE=6.9)

Figure 7. Stationary structures of $(H_2O)_7$ HF at the B3LYP level.

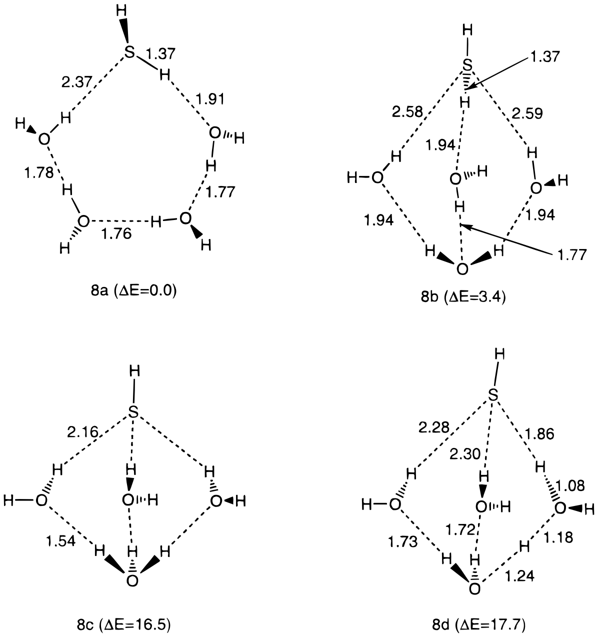

8a (ΔE=0.0) 8b (ΔE=3.4)

8c (ΔE=16.5) 8d (ΔE=17.7)

Figure 8. Stationary structures of $(H_2O)_4$ H_2S at the B3LYP level.

TABLE 4: Relative Energies (kcal mol^{-1}) for $(H_2O)_nH_2S$ Species

		MP2//B3LYP	B3LYP//B3LYP	
		ΔE	ΔE	ΔG
		$(H_2O)_4H_2S$		
ring	(**8a**)	0	0	0
cluster	(**8b**)	3.4	5.0	5.2
ion pair	(**8c**)	16.5	13.8	19.0
transition state	(**8d**)	17.7	15.6	18.0
		$(H_2O)_7H_2S$		
cluster	(**9a**)	0	0	0
ion pair	(**9b**)	5.3	1.9	6.5
transition state	(**9c**)	10.2	6.9	8.1

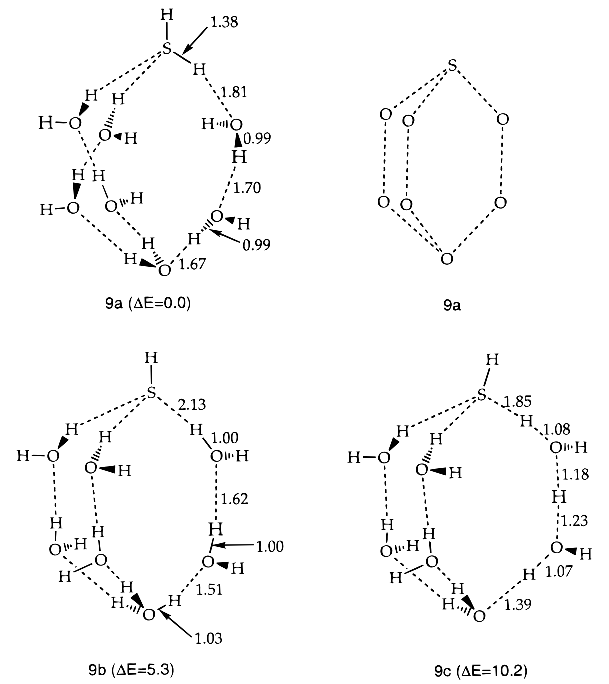

9a (ΔE=0.0) 9a

9b (ΔE=5.3) 9c (ΔE=10.2)

Figure 9. Stationary structures of $(H_2O)_7$ H_2S at the B3LYP level.

acidity and the less polar nature of H_2S. We first note (Table 4) that, as in the case of $(H_2O)_5$, the ring structure is more stable than the cluster. As far as the differences between $(H_2O)_5$ and $(H_2O)_4$ H_2S are concerned, in both neutral clusters of $(H_2O)_4$ H_2S the hydrogen bonds involving H_2S as the proton donor are considerably longer than the corresponding ones in the water pentamer. The energy difference between the neutral and ionic cluster is considerably less by ~5 kcal mol^{-1} than the value for $H_{10}O_5$, reflecting the greater acidity of H_2S compared to H_2O. The transition state (**8d**) that we have identified is earlier than the one associated with proton transfer in the water pentamer, particularly with regards to the formation of the hydroxonium ion. This is in line with the correspondingly lower energy difference between reactants and products.

Turning to the results for the cluster involving seven water molecules (Figure 9, Table 4), we see effects due to the second solvation shell similar to those found for the solvation of HF. Thus, in the neutral cluster, as judged by the hydrogen bond lengths, there are enhanced hydrogen bonding effects, not just to the nearest neighbors but throughout the hydrogen bonding network. In addition, the hydrogen bonded S−H bond in H_2S is slightly lengthened (1.38 compared to 1.37 Å) in the larger cluster. The additional three water molecules also lead to changes in the transition state similar to those found for HF. Thus, the transition state is earlier, particularly with regards to the formation of the hydroxonium ion. Again the free energy difference between the neutral and ion pair cluster is reduced, in this case from 13.8 to 6.5 kcal mol^{-1} at the B3LYP level. However, comparing the MP2 and B3LYP predictions of the energy difference shows, yet again, that DFT preferentially stabilizes the zwitterionic form, in this case by 3.4 kcal mol^{-1}. Correction of our estimate of ΔG at the B3LYP level by this amount results in a free energy of dissociation of 9.9 kcal mol^{-1}, essentially the same as that given from the reported first ionization constant ($pK_1 = 7.04$).[37]

We turn now to the study of water clusters containing larger and more complex solutes. These are of necessity restricted to clusters involving only four water molecules. We chose to study a number of sulfur (IV) species implicated in acid rain formation, building on our previous investigations.[32,38]

$(H_2O)_4$ H_2SO_3. For both sulfurous acid, (H_2SO_3), and the corresponding anion, (HSO_3^-), two possible isomeric forms can in principle exist. Thus, for the anion, the hydrogen atom can

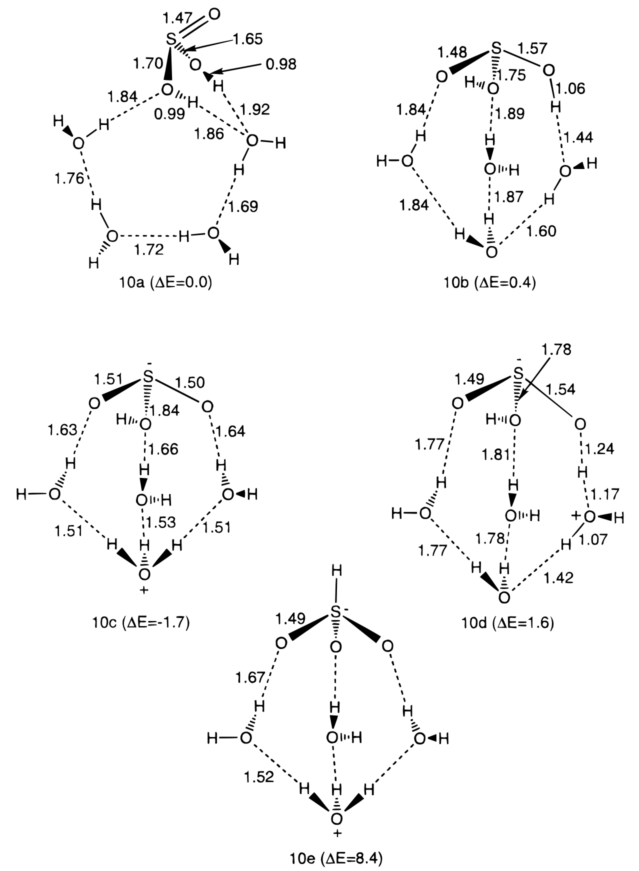
10a (ΔE=0.0) 10b (ΔE=0.4) 10c (ΔE=-1.7) 10d (ΔE=1.6) 10e (ΔE=8.4)

Figure 10. Stationary structures of $(H_2O)_4\ H_2SO_3$ at the B3LYP level.

TABLE 5: Relative Energies (kcal mol^{-1}) for $(H_2O)_4H_2SO_3$ Species

		MP2//B3LYP	B3LYP//B3LYP	
		Δ*E*	Δ*E*	Δ*G*
ring	(**10a**)	0	0.0	0.0
cluster	(**10b**)	0.4	0.1	0.1
ion pair (H−O)	(**10c**)	−1.7	−2.3	0.2
ion pair (H−S)	(**10e**)	8.4	11.6	15.5
transition state	(**10d**)	1.6	0.8	0.7

be bound to the sulfur or to an oxygen atom. It is found experimentally that both forms exist, depending on the condensed-phase environment. In the aqueous phase, the O−H form is favored over the S−H form[39] by 4:1, aided no doubt by the stabilization of −OH due to hydrogen bonding. However, in the solid state,[40] the S−H isomer is found. We have considered both isomeric anions in our cluster studies, but for the neutral acid, only the dihydroxy form has been studied, since, even more so than in the anion, hydrogen bonding to the solvent is expected to stabilize the hydroxy form. Considering the interaction of the neutral and ionized forms of sulfurous acid with four solvating water molecules, we expect there to be many minimum energy structures. We have not attempted to locate all of these, but follow the hydrogen bonding motifs found in our structures with more simple solutes. The stationary structures that we have identified are shown in Figure 10. Thus, for $(H_2O)_4$ H_2SO_3, both a ring (**10a**) and cluster (**10b**) have been found, which at both levels of theory are close in energy (Table 5). The solvated anion pair involving HSO_3^- (**10e**) and $SO_2(OH)^-$ (**10c**) both have the two components of the ion pair separated by a layer of three water molecules, as in the corresponding structures having a smaller solute. As expected, the structure having an S−H bond is considerably higher in energy than that involving the hydroxy anion. If we again take account of the preference of DFT to favor the ion pair, we estimate that the ionized structure has a greater free energy than the solvated neutral acid by ~1 kcal mol^{-1}. This is close to the value of ~2.5 kcal mol^{-1} from the first ionization constant of sulfurous acid ($K_1 = 1.54 \times 10^{-2}$).[37] The transition state (**10d**) is somewhat different from those we have previously found, with proton transfer having largely taken place to a water molecule in the first solvation shell, reflecting the greater acidity of sulfurous acid compared to the other acids we have studied.

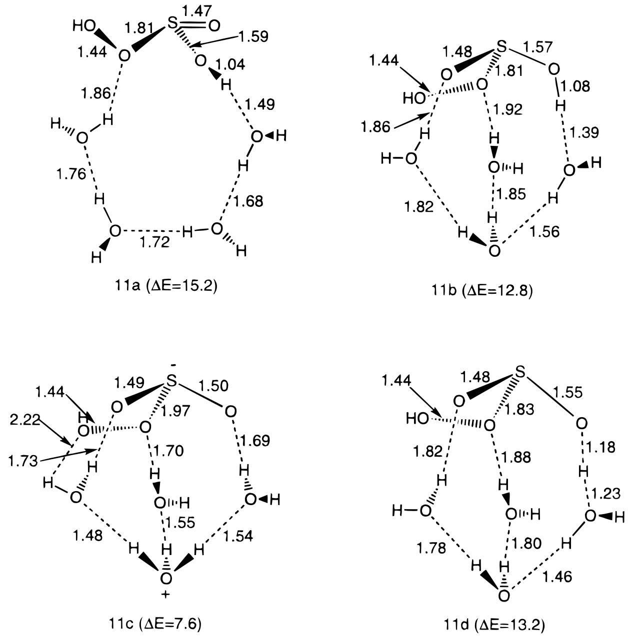
11a (ΔE=15.2) 11b (ΔE=12.8) 11c (ΔE=7.6) 11d (ΔE=13.2)

Figure 11. Stationary structures of $(H_2O)_4{\cdot}HOOSO_2H$ at the B3LYP level.

TABLE 6: Relative Energies (kcal mol^{-1}) of $(H_2O)_4{\cdot}HOOS(OH)O$ and $(H_2O)_4{\cdot}H_2O_2{\cdot}SO_2$ Species

		MP2//B3LYP	B3LYP//B3LYP	
		Δ*E*	Δ*E*	Δ*G*
		$(H_2O)_4{\cdot}H_2O_2{\cdot}SO_2$		
ring	(**12a**)	0	0	0
cluster	(**12b**)	0.4	0.7	2.3
transition state	(**12c**)	9.6	5.2	7.1
		$(H_2O)_4{\cdot}HOOS(OH)O$		
ring	(**11a**)	15.2	8.0	8.5
cluster	(**11b**)	12.8	6.1	7.9
transition state	(**11d**)	13.2	6.2	7.4
ion pair	(**11c**)	7.6	1.7	6.8

$(H_2O)_4{\cdot}HOOSO_2H$ and $(H_2O)_4{\cdot}HOOH{\cdot}SO_2$. The generally accepted mechanism for the oxidation of atmospheric sulfur (IV) species by hydrogen peroxide, leading ultimately to sulfuric acid in the form of acid rain, is through a peroxymonosulfurous species, either $HOOSO_2^-$ or the parent acid.[32] We have obtained stationary structures for the possible reactants, products, and transition states in clusters of four water molecules, as summarized in Figure 11 and Table 6. These structures are similar to those found for smaller solutes. For example, in the zwitterionic form of the acid, the two ions are separated by a layer of three water molecules. As far as the product acid is concerned, at the B3LYP level the cluster having the ionized, zwitterionic form (**11c**) is more stable than the two possible clusters having the acid in its unionized form (**11a**, **11b**). However, in view of the small free energy difference between these two structures and the tendency for DFT to prefer the ionic form, both species may coexist. The corresponding transition state (**11d**) is close to the neutral cluster (**11b**), both

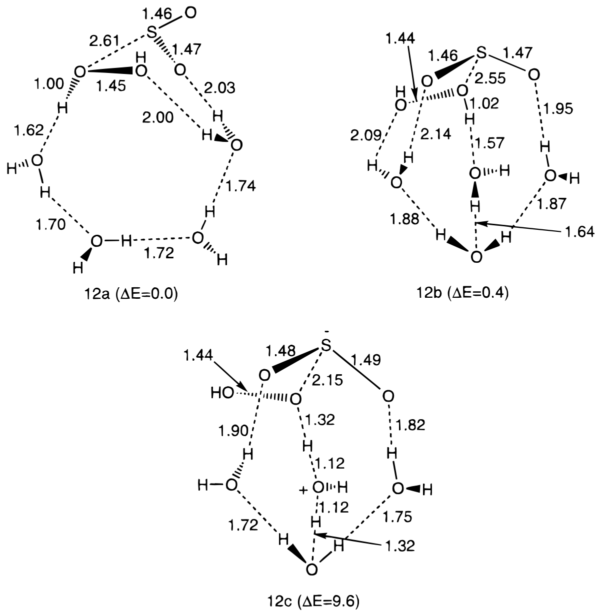

12a (ΔE=0.0) 12b (ΔE=0.4)

12c (ΔE=9.6)

Figure 12. Stationary structures of $(H_2O)_4 \cdot H_2O_2 \cdot SO_2$ at the B3LYP level.

in structure and energy. As we have reported previously,[32] the reaction path involves as reactant a solvated $H_2O_2 \cdot SO_2$ complex (**12a**, **12b**) and a transition state in which a concerted proton shuttle mechanism is apparent (**12c**), leading to formation of the zwitterionic acid product (**11c**). Of the reactant structures (Figure 12), ring (**12a**) or cluster (**12b**), the ring is somewhat more stable. The transition state (**12c**) shows a developing hydroxonium ion, but as in the case of the ionization of sulfurous acid, it is in the first, rather than the second, solvation shell. However, a strong interaction with a water in the second solvation shell, leading to the final zwitterionic product in which the two ions are separated by a layer of water molecules, is clearly evident from the transition state structure.

Conclusions

The complexities of the structure of water itself, and of solutions, particularly those involving ionic solutes, are well-known and have been the subject of continuing experimental and theoretical studies. The energetic and structural features associated with transition states in an aqueous environment are less amenable to experimental study. The advantage of cluster models to probe these processes is that they can be treated at a high level of electronic structure theory, thus avoiding approximations in models that involve low levels of electronic structure theory and force fields. Such clusters can now be of sufficient size that they include at least some of the cooperative effects important in bulk solvation. In all such calculations it is, of course, imperative that a balanced description of the neutral and zwitterionic species be used. We have found that both basis sets and level of correlation must be carefully chosen to avoid some preferential stabilization of the zwitterionic structures. Thus, even with a large basis (6-311+g**), expansion of the basis still further by addition of a fourth s function on the hydrogen (6-311++g**), can alter the nature of the stationary structures. We have found such a situation here for $(H_2O)_3$-HCl, and upon reexamining our previous results[32] for $[H_7O_3{}^+ \cdot HOOSO_2{}^-]$ we find that this zwitterion is no longer a stationary structure when the larger basis is used. A second, general feature is the importance of zero-point effects in determining the relative energetics. These effects tend to be larger when there is favorable hydrogen bonding interactions, thus reducing the free energy difference between different structures.

As far as water itself is concerned, there are changes in the stationary structures on enlarging the cluster, although the energetics are largely unaltered. In particular, the transition state is earlier with respect to the neutral cluster, for the octamer compared to the pentamer so that the transition structure is close to OH^- and a hydroxonium ion in the pentamer, but closer to OH^- plus $H_5O_2{}^+$ for the octamer, reflecting the cooperative nature of the proton-transfer mechanism. Many of the qualitative features found in the studies of pure water clusters are evident from our results for clusters involving other acidic solutes. However, there are quantitative differences that are associated with the varying acidity of the solutes and cluster size. For the solutes studied, the transition states for ionization tend to be earlier for the stronger acids. For the larger clusters with HF and H_2S as solutes, the trend, evident for $(H_2O)_8$, that of an earlier transition state in which a species resembling $H_5O_2{}^+$ can be clearly identified, is even more pronounced, particularly for the more acidic solute H_2S. For yet more acidic solutes, such as H_2SO_3, the ion pair product still involves the separation of the two ions by a layer of water molecules. However, the transition state has a developing hydroxonium ion next to the developing anion (**10d**), which we have found collapses to the ion pair product (**10e**) without a subsequent barrier.

Care must of course be taken if these results obtained for small model clusters were to be extrapolated to larger clusters, which may be more appropriate to describe, for example, atmospherically important reactions in water droplets. Thus, in the calculations described here for the ion pairs and transition states, only part, rather than the whole of the ion is solvated. To extend the present calculations to include more explicit water molecules would be computationally prohibitive. However, the effect of bulk solvation on the clusters can be estimated using a continuum model. Although such an approach has limitations in that explicit hydrogen bonding involving the solvent is not considered, the usefulness of such a model is widely accepted. We have used the SCIPCM[41] variant of the continuum model to estimate the effect of bulk solvent on the energy difference between the cluster (**2b**) and ion pair (**2c**) structures of $(H_2O)_5$. At the B3LYP//B3LYP level, this energy difference, which for the clusters themselves is 17.8 kcal mol^{-1} (Table 1), increased to 19.8 kcal mol^{-1} when bulk solvation is included. This is quite a small change, and it is of interest that it is the unionized cluster that is preferentially solvated. This is due to its greater polarity ($\mu = 3.5$ D) compared to that of the ion pair structure ($\mu = 0.5$ D). The rather small effect that bulk solvation has on the ionization energy is in line with the agreement between our pK_a values calculated for the isolated clusters and experimental bulk values.

Acknowledgment. We thank EPSRC for support of this research.

References and Notes

(1) *Cluster of Atoms and Molecules*; Haberland, H., Ed.; Springer Series in Chemical Physics; Springer: Berlin, 1994; p 56.

(2) Xantheas, S S.; Dunning, T. H. *J. Chem. Phys.* **1993**, *99*, 8774.

(3) (a) McEwan, M. J.; Phillips, L. F. *Chemistry of the Atmosphere*; Edward Arnold: London, 1975. (b) Wayne, R. P. *Chemistry of Atmospheres*; Clarendon Press: Oxford, 1991.

(4) Lear, J. D.; Wasserman, Z. R.; DeGrado, W. F. *Science* **1988**, *240*, 1177. Akeson, M.; Deamer, D. *Biophys. J.* **1991**, *60*, 101. Sangnella, D.; Laasonen, K.; Klein, H. L. *Biophys. J.* **1996**, *71*, 1172. Liu, L.; Brown, M. G.; Saykally, R. J.; Gregory, J. K.; Clary, D. C. *Nature* **1996**, *381*, 501.

(5) Gregory, J. K.; Clary, D. C.; Liu, K.; Brown, M. G.; Saykally, R. J. *Science* **1997**, *275*, 814.

(6) Cheng, H.-P. *J. Phys. Chem. A* **1998**, *102*, 6201.

(7) Tozer, D. J.; Lee, C.; Fitzgerald, G. *J. Chem. Phys.* **1996**, *104*, 5555.

(8) Cardenas, R.; Lagunez-Otero, J.; Flores-Rivero, A. *Int. J. Quantum Chem.* **1998**, *68*, 253.

(9) Pedulla, J. M.; Kim, K.; Jordan, K. D. *Chem. Phys. Lett.* **1998**, *291*, 78.

(10) Gregory, J. K.; Clary, D. C. *J. Chem. Phys.* **1996**, *100*, 18014.

(11) Kim, J.; Lee, J. Y.; Lee, S.; Mhin, B. J.; Kim, K. S. *J. Chem. Phys.* **1995**, *102*, 310.

(12) Xantheas, S. S. *J. Chem. Phys.* **1995**, *102*, 4505.

(13) Quintana, I. M.; Ortiz, W.; Lopez, G. E. *Chem. Phys. Lett.* **1998**, *287*, 429.

(14) Lee, C.; Chen, H.; Fitzgerald, G. *J. Chem. Phys.* **1995**, *102*, 1266.

(15) Lee, C.; Sosa, C.; Novoa, J. *J. Chem. Phys.* **1995**, *103*, 4360.

(16) Wales, D. J.; Walsch, T. R. *J. Chem. Phys.* **1997**, *106*, 7193.

(17) Wales, D. J.; Walsch, T. R. *J. Chem. Phys.* **1996**, *105*, 6957.

(18) Geiger, F. M.; Hicks, J. M.; de Dios, A. C. *J. Phys. Chem. A* **1998**, *102*, 1514.

(19) Ando, K.; Hynes, J. T. *J. Phys. Chem. B* **1997**, *101*, 10464.

(20) Packer, M. J.; Clary, D. C. *J. Phys. Chem.* **1995**, *99*, 14323.

(21) Estrin, D. A.; Kohanoff, J.; Laria, D. H.; Weht, R. O. *Chem. Phys. Lett.* **1997**, *280*, 280.

(22) Re, S.; Osamura, Y.; Suzuki, Y.; Schaefer, H. F. *J. Chem. Phys.* **1998**, *109*, 977.

(23) Lee, C.; Sosa, C.; Planas, M.; Novoa, J. J. *J. Chem. Phys.* **1996**, *104*, 7081.

(24) Planas, M.; Lee, C.; Novoa, J. J. *J. Phys. Chem.* **1996**, *100*, 16495.

(25) Lin, K.; Cruzan, J. D.; Saykally, R. J. *Science* **1996**, *271*, 929.

(26) Kim, K.; Jordan, K. D.; Zwier, T. S. *J. Am. Chem. Soc.* **1994**, *116*, 11568.

(27) Tsai, C. J.; Jordan, K. D. *Chem. Phys. Lett.* **1993**, *213*, 181.

(28) Cieplak, P.; Lybrand, T. P.; Kollman, P. A. *J. Chem. Phys.* **1987**, *86*, 6393.

(29) Perera, L.; Berkowitz, M. L. *J. Chem. Phys.* **1994**, *100*, 3085.

(30) Dang, L. X. *J. Chem. Phys.* **1992**, *96*, 6970.

(31) Bryce, R. A.; Vincent, M. A.; Malcolm, N. O. J.; Hillier, I. H.; Burton, N. A. *J. Chem. Phys.* **1998**, *109*, 3077.

(32) Vincent, M. A.; Palmer. I. J.; Hillier, I. H.; Akhmatskaya, E. *J. Am. Chem. Soc.* **1998**, *120*, 3431.

(33) Trout, B. L.; Parrinello, M. *Chem. Phys. Lett.* **1998**, *288*, 343.

(34) Frisch, M. J.; Trucks, G. W.; Schlegel, H. B.; Gill, P. M. W.; Johnson, B. G.; Robb, M. A.; Cheeseman, J. R.; Keith, T. A.; Petersson, G. A.; Montgomery, J. A.; Raghavachari, K.; Al-Laham, M. A.; Zakrzewski, V. G.; Ortiz, J. V.; Foresman, J. B.; Cioslowski, J.; Stefanov, B. B.; Nanayakkara, A.; Challacombe, M.; Peng, C. Y.; Ayala, P. Y.; Chen, W.; Wong, M. W.; Andres, J. L.; Replogle, E. S.; Gomperts, R.; Martin, R. L.; Fox, D. J.; Binkley, J. S.; Defrees, D. J.; Baker, J.; Stewart, J. P.; Head-Gordon, M.; Gonzalez, C.; Pople, J. A. *Gaussian 94*, revision A.1; Gaussian, Inc., Pittsburgh, PA, 1995.

(35) Jensen, J. O.; Samuels, A. C.; Krishnan, P. N.; Burke, L. A. *Chem. Phys. Lett.* **1997**, *276*, 145.

(36) Koch, T. G.; Banham, S. F.; Sodeau, J. R.; Horn, A. B.; McCoustra, M. R. S.; Chesters, M. A. *J. Geophys. Res.* **1997**, *102*, 1513.

(37) *CRC Handbook of Chemistry and Physics*; Weast, R. C., Ed.; CRC Press: Boca Raton, FL, 1985.

(38) Vincent, M. A.; Palmer, I. J.; Hillier, I. H. *J. Mol. Struct. (THEOCHEM)* **1997**, *394*, 1.

(39) Horner, D. A.; Connick, R. E. *Inorg. Chem.* **1986**, *25*, 2414.

(40) Johanson, L.-G.; Lindqvist, O.; Vannerberg, N.-G. *Acta Crystallogr.* **1980**, *B36*, 2523.

(41) Foresman, J. B.; Keith, T. A.; Wiberg, K. B.; Snoonian, J.; Frisch, M. J. *J. Phys. Chem.* **1996**, *100*, 16098.